



# Observation of Radiative $B$ Meson Decays into Higher Kaonic Resonances (Penguin Mediated $B$ Decays at Belle)

Shohei Nishida\* (Belle Collaboration)

*Department of Physics, Kyoto University, Kitashirakawa-Oiwakecho, Kyoto, Japan*

*E-mail: nishida@scphys.kyoto-u.ac.jp*

ABSTRACT: We have studied radiative  $B$  meson decays into higher kaonic resonances decaying into a two-body or three-body final state, using a data sample of  $21.3 \text{ fb}^{-1}$  recorded at the  $\Upsilon(4S)$  resonance with the Belle detector at KEKB. For the two-body final state, we extract the  $B \rightarrow K_2^*(1430)\gamma$  component from an analysis of the helicity angle distribution, and obtain  $\mathcal{B}(B^0 \rightarrow K_2^*(1430)^0\gamma) = (1.26 \pm 0.66 \pm 0.10) \times 10^{-5}$ . For the three-body final state, we observe a  $B \rightarrow K\pi\pi\gamma$  signal that is consistent with a mixture of  $B \rightarrow K^*\pi\gamma$  and  $B \rightarrow K\rho\gamma$  for the first time.

## 1. Introduction

Radiative  $B$  meson decay through the  $b \rightarrow s\gamma$  process has been one of the most sensitive probes of new physics beyond the Standard Model (SM). The inclusive picture of the  $b \rightarrow s\gamma$  process is well established; however, our knowledge of the exclusive final states in radiative  $B$  meson decays is rather limited. A relativistic form-factor model calculation [1] predicts that more than 20% of the  $b \rightarrow s\gamma$  process should hadronize as kaonic resonances ( $K_X$ ). CLEO has already reported an indication of the  $B \rightarrow K_2^*(1430)\gamma$  signal [2]. Precision measurement of the inclusive  $b \rightarrow s\gamma$  branching fraction will require detailed knowledge of such resonances, for example to model the decay processes into multi-particle final states. In this analysis, we study radiative  $B$  meson decay processes into higher kaonic resonances, which subsequently decay into two-body or three-body final states.

We have analyzed a data sample that contains  $22.8 \times 10^6 B\bar{B}$  events. The data sample corresponds to an integrated luminosity of  $21.3 \text{ fb}^{-1}$  collected at the  $\Upsilon(4S)$  resonance with the Belle detector [3] at the KEKB  $e^+e^-$  collider [4].

\*Speaker.

## 2. Analysis of $B \rightarrow K_2^*(1430)\gamma$

In the  $B \rightarrow K_2^*(1430)\gamma$  analysis, we reconstruct  $K_2^*(1430)$  from  $K^+\pi^-$  (charge conjugate modes are implicitly included) and require the  $K\pi$  invariant mass to be within  $\pm 125 \text{ MeV}/c^2$  of the nominal  $K_2^*(1430)$  value. Then, we combine the  $K_2^*(1430)$  candidate with a high energy (1.8 to 3.4 GeV in the  $\Upsilon(4S)$  rest frame) photon ( $\gamma$ ) candidate inside the acceptance of the barrel calorimeter ( $33^\circ < \theta_\gamma < 128^\circ$ ) to reconstruct a  $B$  meson candidate, and form two independent variables: the beam constrained mass  $M_{bc} \equiv \sqrt{(E_{\text{beam}})^2 - |\vec{p}_{K_X} + \vec{p}_\gamma|^2}$ , and the energy difference  $\Delta E \equiv E_{K_X} + E_\gamma - E_{\text{beam}}$ . We apply a cut of  $-100 \text{ MeV} < \Delta E < 75 \text{ MeV}$ .

To suppress backgrounds from continuum light quark-pair ( $q\bar{q}$ ) production, we apply a likelihood ratio cut where the likelihood ratio is calculated from the  $B$  meson flight direction and an event shape variable which we call SFW [5]. We find that the contribution of the background from other  $B$  meson decays is negligible from Monte Carlo (MC) study. Cross-feed from other  $b \rightarrow s\gamma$  final states is estimated using an inclusive  $b \rightarrow s\gamma$  MC sample, and subtracted from the signal yield.

The  $M_{bc}$  distribution for  $B^0 \rightarrow K_2^*(1430)^0\gamma$  is shown in Fig. 1. By the fit to the  $M_{bc}$  distribution using a sum of a Gaussian function and a threshold-type function (ARGUS function [6]), we obtain  $29.1 \pm 6.7^{+2.4}_{-1.9}$  events, of which the contribution from other  $b \rightarrow s\gamma$  decays is estimated to be  $0.4 \pm 0.3$  events. The event selection efficiency is determined to be  $(6.99 \pm 0.55)\%$  including the sub-decay branching fractions from a MC sample that is calibrated with high statistics control data samples.

In order to distinguish the  $B \rightarrow K_2^*(1430)\gamma$  signal from  $B \rightarrow K^*(1410)\gamma$  and non-resonant decays, we examine the helicity angle distribution for the signal candidates. All three modes have different helicity distributions:  $\cos^2 \theta_{\text{hel}} - \cos^4 \theta_{\text{hel}}$  for  $K_2^*(1430)$ ,  $1 - \cos^2 \theta_{\text{hel}}$  for  $K^*(1410)$  and uniform for non-resonant decay. We divide  $\cos \theta_{\text{hel}}$  into 5 bins, and extract the yield from fits to the  $M_{bc}$  distribution for each bin (Fig. 2). This distribution clearly favors  $B \rightarrow K_2^*(1430)\gamma$ . We fit the  $\cos \theta_{\text{hel}}$  distribution and obtain  $20.1 \pm 10.5$  events for the  $B \rightarrow K_2^*(1430)\gamma$  component. After subtracting other  $b \rightarrow s\gamma$  contributions, this leads to a  $B^0 \rightarrow K_2^*(1430)^0\gamma$  branching fraction of

$$\mathcal{B}(B^0 \rightarrow K_2^*(1430)^0\gamma) = (1.26 \pm 0.66 \pm 0.10) \times 10^{-5}.$$

The background subtracted  $K\pi$  invariant mass distribution for  $B \rightarrow K\pi\gamma$  is obtained by a similar method. In Fig. 3. we see a clear enhancement around  $1.4 \text{ GeV}/c^2$ , which supports the conclusion that the  $B \rightarrow K_2^*(1430)\gamma$  contribution dominates.

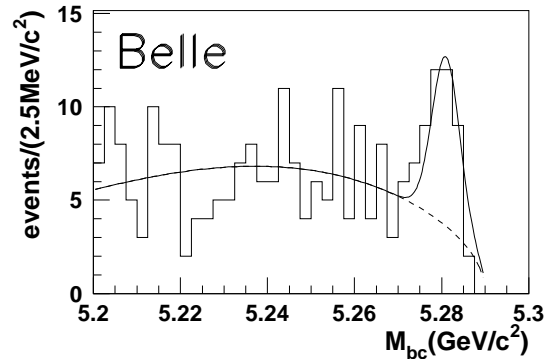


**Figure 1:** The  $M_{bc}$  distributions for  $B^0 \rightarrow K_2^*(1430)^0\gamma$ . The solid line is the fitting result. The background component is shown as the dashed line.

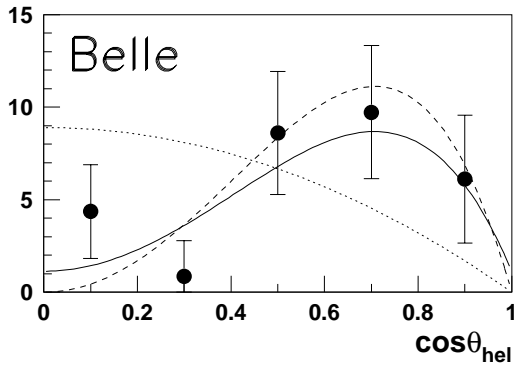


**Figure 2:** The background subtracted  $K_2^*(1430)$  helicity angle distribution. The solid curve is the fitting result. The curve for  $B \rightarrow K_2^*(1430)\gamma$  ( $B \rightarrow K^*(1410)\gamma$ ) is shown as the dashed (dotted) line.

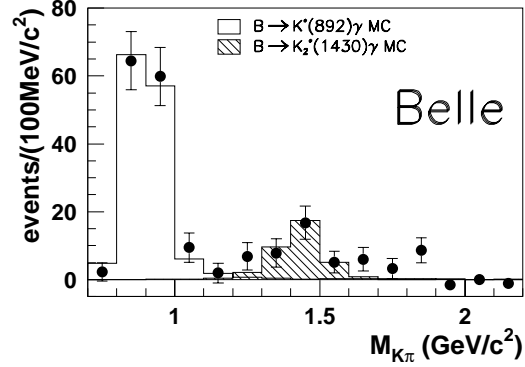


**Figure 3:** The background subtracted  $K\pi$  invariant mass distribution.

### 3. Analysis of $B \rightarrow K_X\gamma \rightarrow K\pi\pi\gamma$

The selection criteria used to reconstruct the  $B \rightarrow K\pi\pi\gamma$  decay are similar to those used in the analysis of  $B \rightarrow K_2^*(1430)\gamma$ . The  $K_X$  candidate is reconstructed from  $K^+\pi^-\pi^+$ , and required to have a mass between  $1.0 \text{ GeV}/c^2$  and  $2.0 \text{ GeV}/c^2$ . The three charged tracks are required to form a vertex.

We select  $B \rightarrow K_X\gamma \rightarrow K^*\pi\gamma$  candidates ( $K^*$  denotes  $K^*(892)$  for simplicity) by requiring the invariant mass of  $K^+\pi^-$  to be within  $\pm 75 \text{ MeV}/c^2$  of the nominal  $K^*$  mass. We obtain  $46.4 \pm 7.3^{+1.6}_{-2.7}$  events from the  $M_{bc}$  distribution (Fig. 4). After subtracting  $B^+ \rightarrow K^+\rho^0\gamma$  or non-resonant contribution using  $M_{K\pi}$  sideband and other  $b \rightarrow s\gamma$  contribution using MC, we obtain a  $B^+ \rightarrow K^{*0}\pi^+\gamma$  yield of  $39.7 \pm 7.4^{+1.7}_{-2.6}$  events.

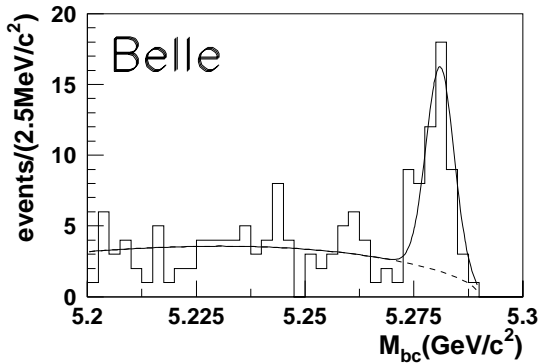


**Figure 4:** The  $M_{bc}$  distribution for  $B \rightarrow K^*\pi\gamma$  candidates.

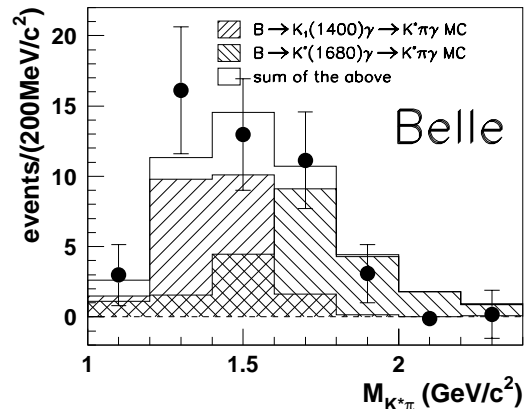


**Figure 5:** The background subtracted  $K\pi\pi$  invariant mass distribution for the  $B \rightarrow K^*\pi\gamma$  analysis.

From the  $K_X$  invariant mass ( $M_{K_X}$ ) distribution (Fig. 5), we observe a broad structure

below  $2.0 \text{ GeV}/c^2$  that can be explained, for example, as a sum of two known resonances around  $1.4 \text{ GeV}/c^2$  and  $1.7 \text{ GeV}/c^2$ , but cannot be explained by a single known resonance or phase space decay. We observe no excess above  $2.0 \text{ GeV}/c^2$ , indicating that the  $M_{K_X} < 2.0 \text{ GeV}/c^2$  cut does not introduce a significant inefficiency.

To estimate the efficiency of  $B \rightarrow K^*\pi\gamma$ , we analyze  $B \rightarrow K_1(1400)\gamma$  and  $B \rightarrow K^*(1680)\gamma$  MC samples, use the mean of the efficiencies as the central value, and assign the difference to the systematic error. As a result, the efficiency becomes  $(3.13 \pm 0.47)\%$  including the other systematic errors. We determine the  $B \rightarrow K^*\pi\gamma$  branching fraction,

$$\mathcal{B}(B \rightarrow K^*\pi\gamma; M_{K^*\pi} < 2.0 \text{ GeV}/c^2) = (5.6 \pm 1.1 \pm 0.9) \times 10^{-5}.$$

There are four known resonances,  $K_1(1270)$ ,  $K_1(1400)$ ,  $K^*(1410)$  and  $K_2^*(1430)$ , that can contribute to the signal around  $M_{K_X} = 1.4 \text{ GeV}/c^2$ . In the region of  $1.2 \text{ GeV}/c^2 < M_{K_X} < 1.6 \text{ GeV}/c^2$ , we obtain  $22.9 \pm 5.1^{+1.0}_{-1.7}$  events from the  $M_{bc}$  distribution, where the  $K_2^*(1430)$  contribution is estimated to be  $2.6 \pm 1.4$  events from our branching fraction measurement. We interpret the signal yield as an upper limit on the weighted sum of the three resonances:  $\frac{1}{2}\mathcal{B}(B \rightarrow K_1(1270)\gamma) + \mathcal{B}(B \rightarrow K_1(1400)\gamma) + \mathcal{B}(B \rightarrow K^*(1410)\gamma) < 5.1 \times 10^{-5}$  (90% C.L.).

Next, we select  $B \rightarrow K_X\gamma \rightarrow K\rho\gamma$  candidates by requiring the invariant mass of the  $\pi^+\pi^-$  combination to be within  $\pm 250 \text{ MeV}/c^2$  of the nominal  $\rho$  mass. To veto  $B \rightarrow K_X\gamma \rightarrow K^*\pi\gamma$  events, we reject a candidate if the invariant  $K^+\pi^-$  mass is within  $\pm 125 \text{ MeV}/c^2$  of the nominal  $K^*$  mass. The  $M_{bc}$  distribution and the  $K_X$  invariant mass distribution are shown in Figs. 6 and 7, respectively. From the  $M_{bc}$  distribution, we obtain a signal yield of  $24.5 \pm 6.4^{+1.2}_{-2.3}$  events. We subtract the contribution of  $2.3 \pm 1.2$  events from other  $b \rightarrow s\gamma$  decays.

The  $M_{K_X}$  spectrum of these events (Fig. 7) shows a large peak around  $1.7 \text{ GeV}/c^2$ . Since there are quite a few resonances around  $1.7 \text{ GeV}/c^2$ , a detailed analysis will be required to disentangle the resonant substructure. The reconstruction efficiency for  $B \rightarrow K\rho\gamma$ , which is  $M_{K_X}$  dependent, is determined to be  $(1.51 \pm 0.25)\%$  by assuming a mixture of  $K_1(1270)$  and  $K^*(1680)$  with a ratio from the  $M_{K_X}$  fit result. So far we find no signal outside the  $\rho$  mass window; neglecting the non-resonant  $K\pi\pi\gamma$  contribution, we determine the  $B \rightarrow K\rho\gamma$  branching fraction,

$$\mathcal{B}(B \rightarrow K\rho\gamma; M_{K\rho} < 2.0 \text{ GeV}/c^2) = (6.5 \pm 1.7^{+1.1}_{-1.2}) \times 10^{-5}.$$

The  $K\rho\gamma$  final state in the mass range around  $1.3 \text{ GeV}/c^2$  is effective for the search of  $B \rightarrow K_1(1270)\gamma$ . We find 4 candidates in the signal box with a background expectation of 1.19 events, when we require  $|M_{K_X} - M_{K_1(1270)}| < 0.1 \text{ GeV}/c^2$ , and obtain an upper limit of  $\mathcal{B}(B \rightarrow K_1(1270)\gamma) < 9.6 \times 10^{-5}$  (90% C.L.).

#### 4. Conclusion

We have searched for radiative  $B$  meson decays into kaonic resonances that decay into a two-body or three-body final states together with a high energy photon. We observe sizable

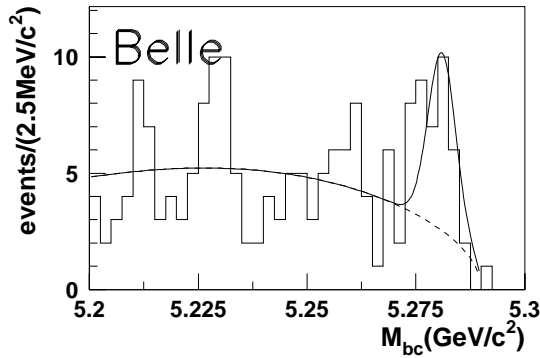


**Figure 6:** The  $M_{bc}$  distribution for  $B \rightarrow K\rho\gamma$  candidates.

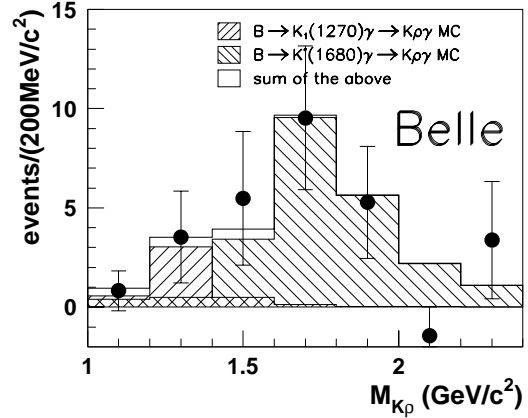


**Figure 7:** The  $K\pi\pi$  invariant mass distribution in the  $B \rightarrow K\rho\gamma$  analysis. Background is subtracted in each bin.

signals in  $B \rightarrow K_2^*(1430)\gamma$ ,  $B \rightarrow K^*\pi\gamma$  and  $B \rightarrow K\rho\gamma$  decays and determine the branching fractions for these channels. The measured branching fractions respectively correspond to about 4%, 17% and 19% of the total  $b \rightarrow s\gamma$  branching fraction [5, 8–10]. Adding 15% from the  $K^*(892)\gamma$  branching fractions, these decay modes sum up to about half of the entire  $b \rightarrow s\gamma$  process.

For the  $K\pi\gamma$  final state, the  $K_2^*(1430)\gamma$  component is separated from a possible  $K^*(1410)\gamma$  or non-resonant contribution using a helicity angle analysis.

For the three-body final states, we observe  $B \rightarrow K^*\pi\gamma$  and  $B \rightarrow K\rho\gamma$  signals separately for the first time; however, the possible contribution of many kaonic resonances prevents us from further identification of such resonances with the current statistics. We find no significant signal for  $B \rightarrow K_1(1270)\gamma$  decay in the  $K\rho\gamma$  final state.

## References

- [1] S.Veseli and M.G.Olsson, Phys. Lett. B **367**, 309 (1996).
- [2] CLEO Collaboration, T.E.Coan *et al.*, Phys. Rev. Lett. **84**, 5283 (2000).
- [3] Belle Collaboration, K. Abe *et al.*, KEK Progress Report 2000-4 (2000), to be published in Nucl. Inst. and Meth. A.
- [4] KEKB B Factory Design Report, KEK Report 95-7 (1995), unpublished; Y. Funakoshi *et al.*, Proc. 2000 European Particle Accelerator Conference, Vienna (2000).
- [5] Belle Collaboration, K.Abe *et al.*, Phys. Lett. B **511**, 151 (2001).
- [6] ARGUS Collaboration, H. Albrecht *et al.*, Phys. Lett. B **241**, 278 (1990).
- [7] Particle Data Group, D.E. Groom *et al.*, Eur. Phys. J. **C15**, 1 (2000).
- [8] K.Chetyrkin, M.Misiak, M.Münz, Phys. Lett. B **400**, 206 (1997); Erratum *ibid.* B **425**, 414 (1998)
- [9] CLEO Collaboration, M.Alam *et al.*, Phys. Rev. Lett. **74**, 2885 (1995).
- [10] ALEPH Collaboration, R.Barate *et al.*, Phys. Lett. B **429**, 196 (1998)